Mechanobiology in Medicine 3 (2025) 100117

Contents lists available at ScienceDirect

Mechanobiology in Medicine

journal homepage: www.sciencedirect.com/journal/mechanobiology-in-medicine

Full Length Article

Tropomodulin1 regulates the biomechanical changes in macrophages induced by matrix stiffness

Yajun Meng [a,b], Amannisa Tuersuntuoheti [a], Siyu Jiang [a,b], Jiayi Xie [c], Zejun Yue [a], Dingwen Xu [d], Xueyu Geng [a], Xiang Lian [e], Lide Xie [b], Lanping Amy Sung [f], Xifu Wang [e,*], Jing Zhou [a,**], Weijuan Yao [a,g,***]

[a] Hemorheology Center, Department of Physiology and Pathophysiology, School of Basic Medical Sciences, Peking University Health Science Center, Beijing 100191, China
[b] Chengde Medical College, Chengde, Hebei Province, 067000, China
[c] Department of Automatic, Tsinghua University, Beijing 100084, China
[d] Department of Clinic, School of Medical Science, Yangzhou Polytechnic College, Yangzhou, Jiangsu Province, 225127, China
[e] Department of Emergency, Beijing Anzhen Hospital, Capital Medical University, Beijing, 100029, China
[f] Department of Bioengineering, University of California, La Jolla, San Diego, 92093, CA, USA
[g] Department of Integration of Chinese and Western Medicine, School of Basic Medical Science, Peking University Health Center, Beijing, 100191, China

ARTICLE INFO

Keywords:
Matrix stiffness
Macrophage
Migration
Rigidity
Cytoskeletal protein

ABSTRACT

The monocyte/macrophage infiltration plays critical roles in the development of atherosclerosis. Arterial stiffness is a cholesterol-independent risk factor for cardiovascular events. The regulation of arterial stiffness on biomechanics of macrophages and its underlying mechanism remains unclear. We prepared polyacrylamide gels with low and high stiffness that corresponded to healthy and diseased blood vessels, respectively. We found that macrophages cultured on stiff matrix had increased rigidity and migration ability compared to those on soft matrix. An actin capping protein, tropomodulin1 (Tmod1) was upregulated in macrophages by stiff matrix and in arteries with high stiffness. Further analyses showed that deficiency of Tmod1 in macrophages completely or partially prevented the changes in actin polymerization, cell adhesion and cell spreading induced by stiff matrix. Overexpression of Tmod1 in macrophages enhanced actin polymerization, cell adhesion and spreading on stiff matrix. Tmod1 was involved in the regulation of vinculin expression and formation of focal adhesion in macrophages on stiff matrix. Finally, the deficiency of Tmod1 in macrophages retarded the formation of atherosclerotic plaques in blood vessels with high matrix stiffness. The results suggest that Tmod1 was a key regulator in macrophage rigidity and migration on stiff substrate. The present work will help us to understand the biomechanical mechanisms for the development of atherosclerosis.

1. Introduction

Atherosclerotic cardiovascular and cerebrovascular diseases, such as myocardial infarction and stroke, are the leading cause of death and disease burden in China and worldwide.[1,2] Hypertension, hyperlipidemia, and diabetes are the major risk factors for atherosclerosis.[3] Atherosclerosis is caused by an inflammatory response triggered by endothelial dysfunction and the accumulation of lipids in the subintima of blood vessels.[4] Blood monocytes enter the vascular wall and differentiate into macrophages and foam cells. In regular inflammatory responses, macrophages migrate out of the site of inflammation when they ingest foreign bodies or pathogens. But in the atherosclerotic sites the macrophages are trapped and further elicit inflammatory response, contributing to the development of atherosclerosis.[5] Studies on the plaque reversal suggest that the regression of atherosclerosis is accompanied by rapid loss of macrophages and the emigration of macrophages to

This article is part of a special issue entitled: Cardiovascular Mechano published in Mechanobiology in Medicine.

* Corresponding author.
** Corresponding author.
*** Corresponding author. Hemorheology Center, Department of Physiology and Pathophysiology, School of Basic Medical Sciences, Peking University Health Science Center, Beijing, 100191, China.
E-mail addresses: wxf0439@163.com (X. Wang), jzhou@bjmu.edu.cn (J. Zhou), weijuanyao@bjmu.edu.cn (W. Yao).

https://doi.org/10.1016/j.mbm.2025.100117
Received 1 October 2024; Received in revised form 14 January 2025; Accepted 13 February 2025
Available online 20 February 2025

lymph nodes.[6] Therefore, it is of importance to explore the mechanisms related to the change in macrophage migration in diseased blood vessels.

As with all types of migratory cells, macrophage migration depends on the biomechanical properties of the cells, which would affect the efficiency, speed, and the distance of cell migration.[7] By using micropipette aspiration technique, researchers found that macrophages isolated from atherosclerotic plaques in rabbits fed with high-fat diet had a higher elastic moduli and poor deformability than those isolated from normal arteries.[8] This suggests that the mechanical properties of macrophages were changed in disease blood vessels.

The mechanical alteration in macrophages may be caused by the microenvironment in the diseased blood vessels, such as lipid content, vascular stiffness,[9] and cyclic strain.[10] In a variety of vascular diseases, the change of composition, degradation, and remodeling of the extracellular matrix (ECM) are the hallmarks for disease development, which result to the vascular stiffening.[11] Researchers found that the content of fibronectin and collagen increased in plaque lesions, while laminin and elastin content decreased. The alteration in ECM components promotes arterial sclerosis and the development of coronary artery disease.[12] By nanoindentation, we found that the stiffness for healthy human carotid artery was ~2.3 kPa, while the stiffness of the calcified region of the samples from patients undergoing carotid endarterectomy was as high as 23.94 kPa.[13] By atom force microscope, researchers found that the aortic stiffness was ~5 kPa in healthy mice, but the aortic stiffness was augmented to ~28 kPa in *ApoE*$^{-/-}$ mice due to atherosclerosis.[9,14] The results indicate that vascular stiffening occurs in atherosclerosis, and thus may influence the mechanical behavior of macrophages.

In *in vitro* experiments, when macrophages were cultured on different substrates with stiffness ranging from soft to hard, the morphology of the cells changed from round to flat, and cell spreading, adhesion, and cell stiffness all increased.[15] In *ApoE*$^{-/-}$ mice, researchers found that the mice had high vascular stiffness because of the excessive matrix proteins produced by vascular smooth muscle cells due to the absence of ApoE. When vascular stiffness was reduced with lysyl oxidase inhibitor BAPN, the area of arterial plaques and the number of macrophages in the plaques were significantly lower than those of the control *ApoE*$^{-/-}$ mice.[9] These results indicate that matrix stiffness has a profound effect on macrophage motility. It has been shown that the degree of actin polymerization is a major determinant of macrophage rigidity.[16] Actin polymerization, myosin activity, and Rho-mediated contractility determine the migration of monocyte and macrophage.[17,18] But the underlying molecular mechanisms how matrix stiffness regulates the rigidity and migration of macrophages remain unclear.

Tropomodulin1 (Tmod1) is an actin capping protein at the slow-growing end of actin filaments, slowing down the depolymerization of actin filaments.[19] In erythrocytes and cardiomyocytes, Tmod1 plays an essential role in the mechanical properties and the contractile capacity of cells by regulating the assembly and the length of actin filament.[20,21] The complete knockout of Tmod1 results in the death of mice at 9.5 days in the embryonic stage because of non-contractile heart tube, accumulation of mechanically weakened primitive erythroid cells, and failure of primary capillary plexuses to remodel into vitelline vessels.[20] Tmod1 was also shown to be related to the activation and distribution of focal adhesion molecules in cardiomyocytes.[22]

In the present study, we found that Tmod1 expression responded to matrix stiffness in both macrophages and vascular wall. Deficiency of Tmod1 in macrophages eliminated the changes in actin polymerization, cell adhesion and spreading induced by stiff matrix. Overexpression of Tmod1 in macrophages enhanced actin polymerization, cell adhesion and spreading on stiff matrix. Tmod1 was involved in the regulation of vinculin expression and formation of focal adhesion in macrophages. Finally, the deficiency of Tmod1 in macrophages retarded the formation of atherosclerotic plaques in blood vessels with high matrix stiffness. Our results suggest that Tmod1 was a key regulator in macrophage rigidity and migration on stiff substrate.

2. Materials and methods

2.1. Antibodies, reagents, and animals

Anti-Tmod1 antibody was prepared by Abmax (Beijing, China). The antibody for the cluster of differentiation 36 (CD36) antibody was purchased from Bioss Antibodies (Beijing, China). Antibody for glyceraldehyde-3-phosphate dehydrogenase (GAPDH) and 4′,6-diamidino-2-phenylindole (DAPI) were purchased from Beyotime (Shanghai, China). Anti-vinculin antibody was from Sigma (St. Louis, MO). The adenovirus for Tmod1 (Ad-Tmod1) and its control adenovirus, Ad-null, were prepared by Sinogenomax (Beijing, China). Rhodamine-phalloidin was from Invitrogen (Carlsbad, CA).

TOT/Tmod1$^{-/-}$ mouse was created in Dr. L. Amy Sung's lab at University of California, San Diego.[21] The mouse line was bred from *Tmod1*$^{+/-}$ mouse and TOT mouse (a Transgenic mouse with Over-expressing Tmod1 in the heart). Wild type C57/BL6J mice and male *ApoE*$^{-/-}$ mice were purchased from the animal department of Peking University Health Science Center. All mice were kept in the specific-pathogen-free room of Peking University Health Science Center. High fat diet containing 20 % fat and 1.25 % cholesterol was purchased from Research diets, Inc. (USA). The selective lysyl oxidase inhibitor, BAPN, was purchased from Sigma (St. Louis, MO). For arterial softening mouse model, *ApoE*$^{-/-}$ mice were divided into four groups: PBS injection and chow diet (PBS+ND) group, PBS injection and high fat diet (PBS+HFD) group, BAPN injection and chow diet (BAPN+ND) group, and BAPN injection and high fat diet (BAPN+HFD) group. The animal protocol (#HL2021172) was approved by Animal Care Committee of Peaking University Health Science Center.

2.2. Cell culture

Raw264.7 cells, a mouse mononuclear macrophage leukemia cell line, were cultured in high glucose (4.5 g/L) Dulbecco's modified eagle medium (DMEM) supplemented with 10 % fetal bovine serum (FBS) and antibiotics in an incubator with 37 °C and 5 % CO_2. When reaching 90 % confluency, the cells were blown off by repeated pipetting and passaged to a new petri dish.

2.3. Isolation of murine peritoneal macrophages

Wild type C57BL/6J and *TOT/Tmod1*$^{-/-}$ mice (6–8 weeks) were intraperitoneally injected with 2 mL of 4 % thioglycollate broth. Three days later the lavage was collected by injecting cold PBS into peritoneal cavity. The peritoneal exudate cells were centrifuged at 400×*g* for 10 min and resuspended in cold RPMI-1640 supplemented with 10 % FBS.

2.4. Infection of adenovirus

Raw264.7 cells (2×10^5 cells for each well) were seeded in a six-well plate. After the cells completely adhered, one mL of complete culture medium containing adenovirus Ad-Null or Ad-Tmod1 (200 Multiplicity of Infection) was added into each well. After 24 h of infection, equal volume of complete culture medium was added, and the cells were cultured for another 24 h.

2.5. Transfection of small interfering RNA (siRNA)

The siRNA sequence 5′-GGAAUUUAAGGACCGAGAA-3′ that targets mouse Tmod1 was designed using BLOCK-iT™ RNAi Designer (Thermo Fisher Scientific) and synthesized from RiboBio (Guangzhou, China). A scramble siRNA was purchased from RiboBio. Raw264.7 cells were transfected with 10 nM siRNA by using riboFECT CP Transfection Kit (RiboBio) for 24–48 h.

2.6. Preparation of polyacrylamide gels with various stiffness

Polyacrylamide (PA) gels were prepared by mixing 40 % w/v acrylamide and 2 % w/v bisacrylamide stock solutions with water.[23] Gels with stiffness of 2.61 ± 0.82 and 19.66 ± 1.19 kPa were obtained by manipulating the final concentrations of bisacrylamide (0.048 % and 0.264 %, respectively). After degassing, the mixture was added with 1/10 volume of 10 % w/v ammonium persulfate and 1/100 volume of TEMED (Sigma). About 40 μL of mixture was dropped on a glass slide and covered with a pre-activated cover glass. The cast was placed in UV radiation for 1–2 h and then the cover glass was removed. The gel surface was added with the heterobifunctional crosslinker sulfo-SANPAH (0.5 mg/mL in PBS) and then exposed to 264 nm UV light. After sulfo-SANPAH was removed, the gel was coated with 800 μL of type I collagen (0.2 mg/mL, from rat tail, Corning) for 1 h.

2.7. Measurement of cell and matrix stiffness by nanoindenter

An optical fiber-based nanoindenter (Optics11, Amsterdam, Netherlands) was used to measure the mechanical properties of cells and PA gels. A probe with 0.045 N/m spring constant and 5 μm spherical indentation tip was installed on the PIUMA indentation control driver. The PA gels with or without cells were placed on the bottom of a Petri dish containing culture medium. Under microscope, the nanoindenter tip was located on top of the gels or cells. During the indentation process, the tip was brought into contact with the gel or cell surface and indentation was loaded and the load-time data was recorded. The indentation depth was controlled to 10 μm and the loading and unloading time was set to 2 s. The load displacement curves were fit using Hertz sphrical indentation model and the reduced Young's modulus of gels or cells were calculated. The mean Young's modulus was obtained from 20 to 30 measurements for each PA gel. The Young's modulus for individual cell was derived from one measurement. At least three independent tests were performed.

2.8. Protein extraction and western blotting

To extract proteins from cells, the cells were lysed by RIPA lysis buffer containing 1 mM of phenylmethylsulfonyl fluoride (PMSF) and phosphatase inhibitor cocktail (Applygen, Beijing, China). To extract proteins from blood vessels, the vessels were placed in an Eppendorf tube containing RIPA lysis buffer and cut into small pieces. Then the pieces were transferred into a homogenizer and homogenized on ice. Total proteins were obtained by centrifuging the lysates or homogenates for 10 min or 30 min at 12000×*g* at 4 °C. The protein concentration was quantified with a BCA protein assay kit (Applygen). About 60 μg protein was separated in a 10 % SDS polyacrylamide gel and then transferred onto a PVDF membrane. The membrane was blocked with 5 % non-fat milk and incubated with primary antibodies for overnight at 4 °C. After washing, the membrane was incubated with HRP-conjugated secondary antibodies at room temperature for 1 h. The protein bands were visualized by using an enhanced chemiluminescence (ECL) detection kit (Engreen Biosystem Co., Ltd, Beijing, China). The images were obtained on an Odyssey scanner. The membrane was stripped in the stripping buffer containing β-mercaptoethanol for 15 min at 50 °C before it was used to detect the proteins on the same membrane.

2.9. Real-time quantitative PCR

Total RNA was isolated from cells using RNAtrip reagent (Applygen) and then reverse transcribed into cDNA using RevertAid First Strand cDNA Synthesis Kit (Thermo Fisher Scientific). Real-time quantitative PCR (RT-qPCR) was performed on Mx 3000 Multiplex Quantitative PCR system (Stratagene) using EvaGreen qPCR Master Mix-low Rox (Abm). The primer sequences of murine Tmod1 were 5′-GACACAGCCTCACACAATGT-3’/5′-CTTGGTGGTCTGATCCTTCT-3’. GAPDH was used as an internal control and the primer sequences were 5′-ACCACAGTCCATGCCATCAC-3’/5′-TCCACCACCCTGTTGCTGTA-3’. A relative fold change in the gene expression was calculated using the method of $2^{-\triangle\triangle Ct}$.

2.10. Detection of F-actin by flow cytometry and confocal microscopy

Cells cultured on PA gels were blown off by repetitive pipetting and cell aggregates were filtered using a 400-mesh cell strainer (Corning). After being washed, the cells were fixed in 4 % paraformaldehyde (PFA) for 20 min and then permeabilized in 0.25 % Triton X-100 for 15 min. The cells were blocked with 3 % bovine serum albumin (BSA) solution for 20 min and stained by rhodamine phalloidin (Thermo Fisher Scientific) in the dark at 37 °C. Then the cells were resuspended in PBS and the mean fluorescence intensity was measured using a BD FACS Calibur. To detect F-actin by confocal microscopy, cells on PA gels were directly fixed in 4 % PFA without blowing and stained with rhodamine phalloidin by following the same protocol. The nuclei were counterstained with 4′,6-diamidino-2-phenylindole (DAPI). The cells were photographed on an SP8 LIGHTENING confocal microscope (Leica, Germany) under the same excitation intensity. The fluorescence intensity of F-actin for each image was analyzed by using Image J (NIH).

2.11. Immunofuorescence staining

Cells cultured on PA gels were washed in PBS and fixed in 4 % paraformaldehyde for 20 min at 4 °C. Then the cells were permeabilized in 0.25 % Triton X-100 for 15 min and blocked with 3 % BSA for 1 h at room temperature (RT). The cells were incubated in the blocking solution containing primary antibodies overnight at 4 °C. After being washed for 3 times in PBS, the cells were stained with tetramethylrhodamine (TRITC)-conjugated secondary antibodies at RT for 1 h. The nuclei were counterstained with DAPI for 10 min and then the cells were mounted in antifade mounting medium. The fluorescence images were taken by using an SP8 LIGHTENING confocal microscope.

2.12. Live cell imaging

The live cell imaging for Raw264.7 cells cultured on PA gels was performed with Olympus FV3000 microscope (Japan) equipped with a heater to maintain the temperature at 37 °C. Multiple images were acquired at a single position from each sample every 1 min for 6 h. The videos were assembled from the serial 361 images and imported to Fiji software[24] by using FFMPEG plugin. The TrackMate plugin was used to track the individual cells throughout the video to quantify the total distance traveled.

2.13. Cell adhesion assay

Equal number of cells were plated on PA gels with various stiffness for 30 min. The non-adhered cells were gently washed by PBS and the adhered cells were stained with DAPI. The fluorescence images were taken under an epifluorescence microscope (Olympus, Japan) under 20 × objective. Total of 20 fields were randomly chosen to count the number of adherent cells.

2.14. Cell spreading assay

About 1×10^5 cells were plated onto PA gels with different stiffness for 2 and 6 h. Then the cells were gently washed with PBS and fixed in 4 % PFA. After being permeabilized and blocked in 0.25 % Triton X-100 and 3 % BSA, the cells were stained with rhodamine phalloidin. The nuclei were counterstained with DAPI. The fluorescence images and the differential interference contrast (DIC) images were taken on Leica DM5000 B microscope (Germany). About 20 cells were randomly selected and their spreading areas were measured by using Image J.

2.15. Bone marrow transplantation and analysis of atherosclerosis

Male *ApoE*$^{-/-}$ mice (8 weeks old) were subjected to 1000 rad of total body irradiation followed by reconstitution with 5 × 10^6 bone marrow cells from wild type or *TOT/Tmod1*$^{-/-}$ mice via tail veil injection. After 6 weeks of reconstitution on chow diet, PBS or BAPN (333 mg/kg) were intraperitoneally injected daily for 8 weeks. The body weights of the mice were measured every week. By the end of 8 weeks, the mice were anesthetized by isoflurane gas and blood was collected from inner canthus and used for the measurement of total cholesterol and triglyceride. The mice were perfused with PBS followed by 4 % paraformaldehyde and hearts were collected. Frozen sections with 10-μm thickness were cut from aortic roots and H&E staining and oil red O staining were performed. The images were taken on a BDS 400 inverted microscope (Optec, Chongqing, China) equipped with a CCD camera. The areas of atherosclerotic lesion were measured by using Image J.

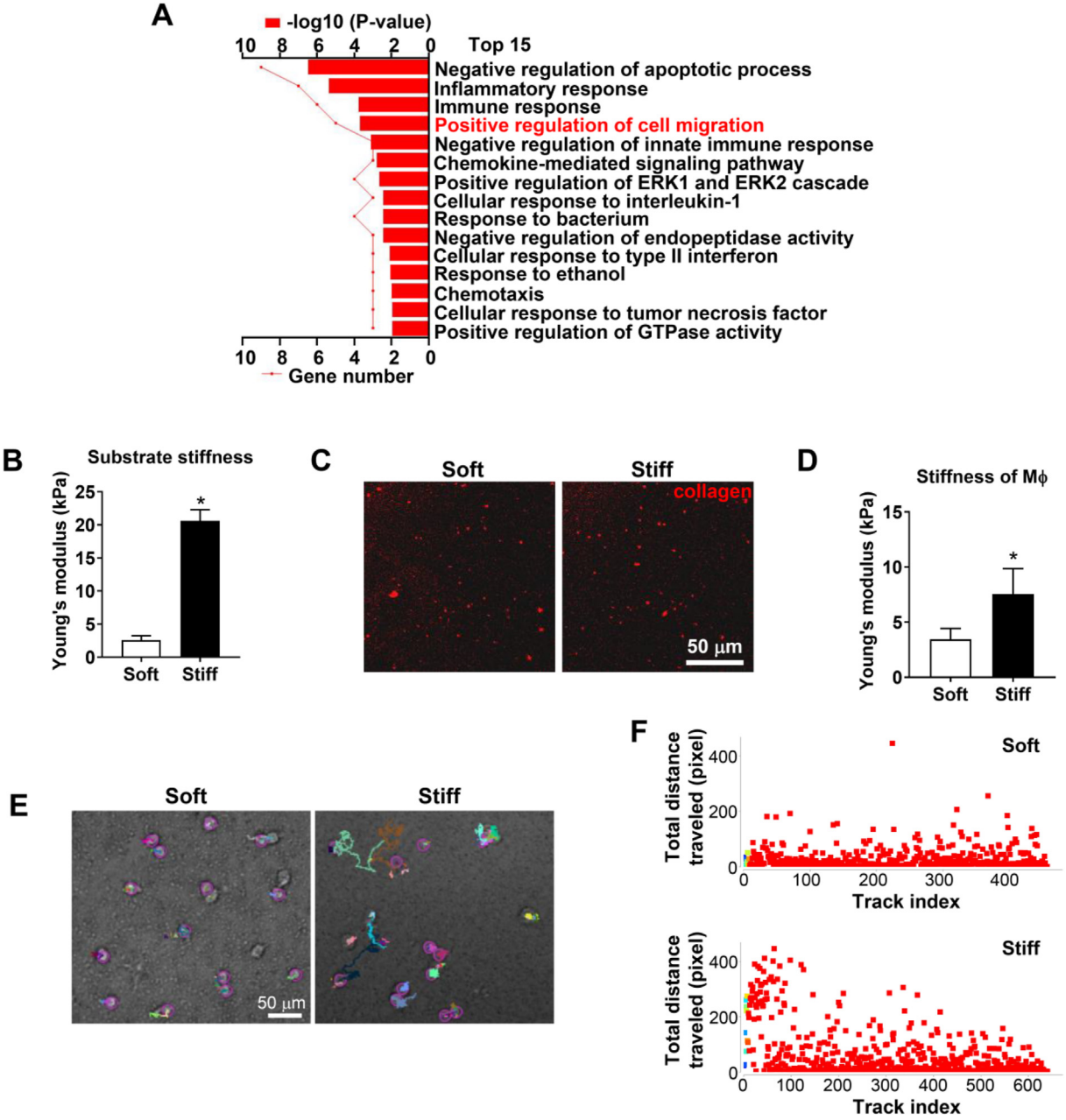

Fig. 1. Macrophage rigidity and migration are increased by stiff matrix. (A) The gene ontology analysis on transcriptional profile (GSE36878). The top 10 most enriched gene ontology (GO) terms were shown for the upregulated genes in macrophages cultured on stiff (150 kPa) polyacrylamide (PA) gel as compared with cells cultured on soft (1.2 kPa) PA gel. **(B)** The stiffness of soft and stiff PA gels as measured by a nanoindenter. The soft and stiff gels had predicted stiffness of 2 kPa and 20 kPa, respectively. The measurements were done at multiple spots on each gel. The Young's modulus for each spot was calculated. n = 4 replicated gels with 5 spots were measured for each gel. **(C)** The immunofluorescence staining of type I collagen (red) on soft and stiff PA gels. **(D)** The stiffness of Raw264.7 cells that cultured on soft (2 kPa) and stiff (20 kPa) PA gels as measured by a nanoindenter. n = ~20 cells for each group. **(E–F)** The live cell imaging for Raw264.7 cells cultured on soft and stiff PA gels **(E)**. The imaging was taken every min for 6 h. The colored lines are drawn using Trackmate plugin in Fiji software and indicate the migrating tracks for individual cells. The total distance traveled (in pixel) was obtained by Trackmate plugin **(F)**. Data in **(B)** and **(D)** were analyzed by Student's *t*-test. *: $P < 0.05$.

2.16. Measurement of total cholesterole and triglyceride

The blood was taken from *ApoE*$^{-/-}$ mice and the plasma was separated by centrifugation. The levels of total cholesterol and triglyceride were measured using Total cholesterol and Triglyceride assay kits (Nanjing Jiancheng Bioengineering Institute, Nanjing, China).

2.17. Statistical analysis

The data was expressed as mean ± standard error of mean (SEM) from at least 3 biological replicates or 5 mice. The statistical analyses were performed using GraphPad Prism 10.0. The paired or unpaired, two-tailed Student's *t*-test was used to compare the difference between two

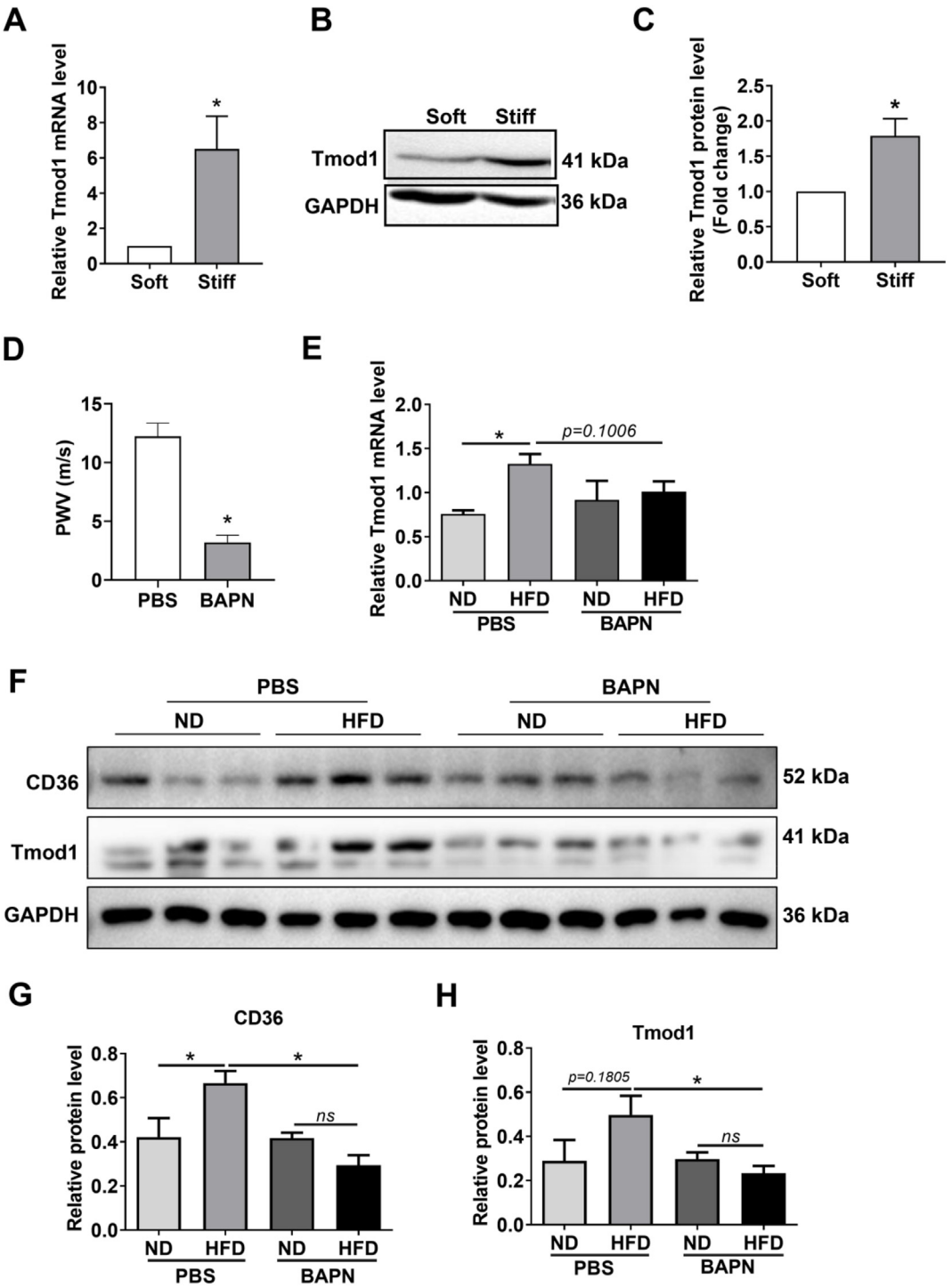

Fig. 2. Tmod1 is upregulated in macrophages in response to stiff matrix. (A–C) The detection of Tmod1 expression at mRNA and protein levels in macrophages cultured on soft (2 kPa) and stiff (20 kPa) PA gels by quantitative RT-PCR **(A)** and western blotting **(B–C)**. The representative blots were shown in **(B)** and the semi-quantification data was shown in **(C)**. n = 3 biological replicates. **(D)** The pulse wave velocities (PWV) of arteries in *ApoE*$^{-/-}$ mice which were injected with phosphate buffered saline (PBS) or lysyl oxidase inhibitor BAPN. n = 3 mice. **(E–H)** The mRNA expression of Tmod1 (E) and protein levels of CD36 and Tmod1 **(F)** in arteries of *ApoE*$^{-/-}$ mice that were injected with PBS or BAPN and fed with normal diet (ND) or high-fat diet (HFD). The representative blots were shown in **(F)**. The semi-quantification data for CD36 and Tmod1 were shown in **(G)** and **(H)**, respectively. n = 3–4 mice. Data in **(A)**, **(C)** and **(D)** were analyzed by Student's *t*-test. Data in **(E)**, **(G)**, and **(H)** were analyzed by two-way ANOVA test followed by the Tukey's multiple comparisons test. *: $P < 0.05$, ns: no significance.

groups. Two-way ANOVA was used to compare the difference among multiple groups followed by Tukey's post hoc analyses. P value of <0.05 was considered statistically significant.

3. Results

3.1. The elastic moduli and migration ability of macrophages are increased on stiff matrix

To obtain a general idea about how macrophages respond to stiff matrix, we first analyzed a transcriptional profile (GSE36878) found in Gene Expression Omnibus (GEO) dataset repository, in which Raw264.7 cells were cultured on polyacrylamide (PA) gels with stiffness of 1.2 kPa and 150 kPa, respectively, for 18 h[16]. The differentially expressed genes were identified and subjected to the gene ontology (GO) analysis. The results showed that, among the upregulated genes, those related to biological processes, such as inflammatory response, immune response, and positive regulation of cell migration, etc., were significantly enriched (Fig. 1A). This suggests that high matrix stiffness would change the inflammatory state and migration ability of macrophages.

We next hypothesized that stiff matrix in diseased blood vessels could also affect the mechanical properties and migration ability of macrophages. We prepared type I collagen-coated soft (2 kPa) and stiff (20 kPa) PA gels whose stiffness corresponded to those of healthy and diseased vessels, respectively.[13] The Young's moduli of soft and stiff PA gels as measured by using nanoindenter were 2.57 ± 0.68 and 20.62 ± 1.66 kPa, respectively, which were consistent with the predicted stiffness (Fig. 1B). The densities of collagens on soft and stiff gels were examined by immunostaining. The results showed that collagens were evenly coated on the gels and the densities of collagens were comparable between soft and stiff gels (Fig. 1C). The Raw264.7 cells were cultured on soft and stiff PA gels and the Young's moduli were measured by the same method. The results showed that cells cultured on soft gels had smaller Young's moduli than those cultured on stiff gels (3.44 ± 0.99 vs 7.56 ± 2.29 kPa) (Fig. 1D), suggesting that macrophages would become less deformable in the stiff microenvironment of diseased blood vessels.

We then evaluated the migration ability of macrophages on soft and stiff PA gels by live cell imaging. It was found that the total distances traveled for majority of cells cultured on soft gels were less than 200 pixels, while those for a great portion of cells cultured on stiff gels were between 200 and 400 pixels (Fig. 1E and F), suggesting that cells on stiff gels migrated faster than those on soft gels.

3.2. Tmod1 is upregulated in macrophages in response to stiff matrix

Since actin polymerization plays a critical role in macrophage migration on both 2D surface and 3D matrix,[14,18] actin binding proteins that are involved in actin polymerization may be regulated by matrix stiffness. We detected the expression of Tmod1, an actin capping protein that prevents the depolymerization of actin filaments, in macrophages cultured on soft (2 kPa) and stiff (20 kPa) PA gels. Quantitative PCR and western blotting data showed that the expression of Tmod1 was upregulated by high matrix stiffness by ~6-flod and ~1.8-fold at mRNA and protein levels, respectively (Fig. 2A-C). The result suggests that Tmod1 expression in macrophage was mechanosensitive.

It has been shown that the development of atherosclerotic plaque leads to the increase in the vascular stiffness in both human and mouse.[13,25] In addition, an irreversible inhibitor of lysyl oxidase, β-aminopropionitrile monofumarate (BAPN) could be used to reduce the vascular stiffness in mice.[9] Therefore, *ApoE*$^{-/-}$ mice was fed with high-fat diet (HFD) to induce atherosclerosis and increase vascular stiffness. The mice were injected with BAPN for 8 weeks to reduce vascular stiffness, which was demonstrated by pulse wave velocity (PWV) measurement. The results showed that PWVs for aortas of BAPN-treated mice were much lower than those for phosphate-buffered saline (PBS)-treated mice (Fig. 2D). Quantitative PCR showed that Tmod1 expression increased in the aortas of HFD-fed and PBS-treated mice as compared to PBS-treated chow diet-fed mice or BAPN-treated HFD-fed mice (Fig. 2E). The protein levels of Tmod1 and CD36, a scavenger receptor used to indicate the formation of plaques, changed in a similar pattern as the mRNA level of Tmod1 (Fig. 2E-G). Data suggests that Tmod1 was upregulated *in vivo* as aortas became stiffer.

3.3. Deficiency of Tmod1 in macrophages eliminates the changes in actin polymerization, cell adhesion and spreading induced by stiff matrix

Since Tmod1 was upregulated by stiff matrix in macrophages, we next sought to examine the roles of Tmod1 in the alterations induced by stiff matrix. The expression of Tmod1 was knocked down by siRNA in Raw264.7 cells (Fig. 3A and B). The actin polymerization, cell adhesion, and cell spreading, three processes closely related to macrophage rigidity and migration, were evaluated. We first stained the cells with phalloidin to label polymerized actin filaments and quantified its mean fluorescence intensity by flow cytometry. The data showed that macrophages had higher level of actin polymerization on stiff matrix than on soft matrix. But when Tmod1 was knocked down, the level of actin polymerization decreased on both soft and stiff matrix, importantly, the difference between soft and stiff matrix was eliminated (Fig. 3C and D). This suggests that Tmod1 was critical for actin polymerization induced by stiff matrix in macrophages.

When cells migrate, cells need to adhere to the matrix and then spread and stretch out podosome. We found that macrophages tended to adhere more easily on stiff matrix than on soft matrix (Fig. 3E and F). When Tmod1 was knocked down, the adhesion ability of macrophages was significantly reduced on both soft and stiff PA gels. Importantly, the knockdown of Tmod1 eliminated the difference of cell adhesion between soft and stiff matrix (Fig. 3E and F), suggesting that Tmod1 had an important role in the adhesion of macrophages.

To evaluate the cell spreading, we plated macrophages with or without Tmod1 knocked down on soft and stiff matrix for 2 and 6 h. The cells were stained by phalloidin and examined on differential interference contrast (DIC) microscope and cell areas were quantified. The data showed that on stiff matrix, macrophages spread faster than on soft matrix, which resulted to larger cell areas and more podosome formation (Fig. 3G and H). When Tmod1 was knocked down, the spreading speed and podosome formation were significantly decreased, although cell areas could still increase as time went by (Fig. 3G and H). These data indicate that Tmod1 played an important role in macrophage rigidity and migration.

3.4. Overexpression of Tmod1 in macrophages enhances actin polymerization, cell adhesion and spreading on stiff matrix

We next explored the effects of Tmod1 overexpression on actin polymerization, cell adhesion, and spreading in macrophages cultured on matrix with different stiffness. We used adenovirus to infect Raw264.7 cells and qPCR and western blotting data validated the successful overexpression of Tmod1 (Fig. 4A and B). Flow cytometry data showed that overexpression of Tmod1 led to more actin polymerization in macrophages and importantly, it had a synergistic effect with stiff matrix on actin polymerization (Fig. 4C and D).

We also measured the cell adhesion and spreading in macrophages with Tmod1 overexpression. The results showed that overexpression of Tmod1 increased the adhesion ability of macrophages on both soft and stiff matrix. Among all the groups, the adhesion ability was the highest in macrophages which overexpressed Tmod1 and cultured on stiff matrix (Fig. 4E and F). Similarly, overexpression of Tmod1 enhanced the spreading of macrophages on both soft and stiff matrix. By 6 h, macrophages which overexpressed Tmod1 and cultured on stiff matrix had the largest cell areas and more podosome formation among the groups (Fig. 4G and H). Our results suggest that the overexpression of Tmod1 could enhance actin polymerization, cell adhesion and spreading in macrophages on stiff matrix.

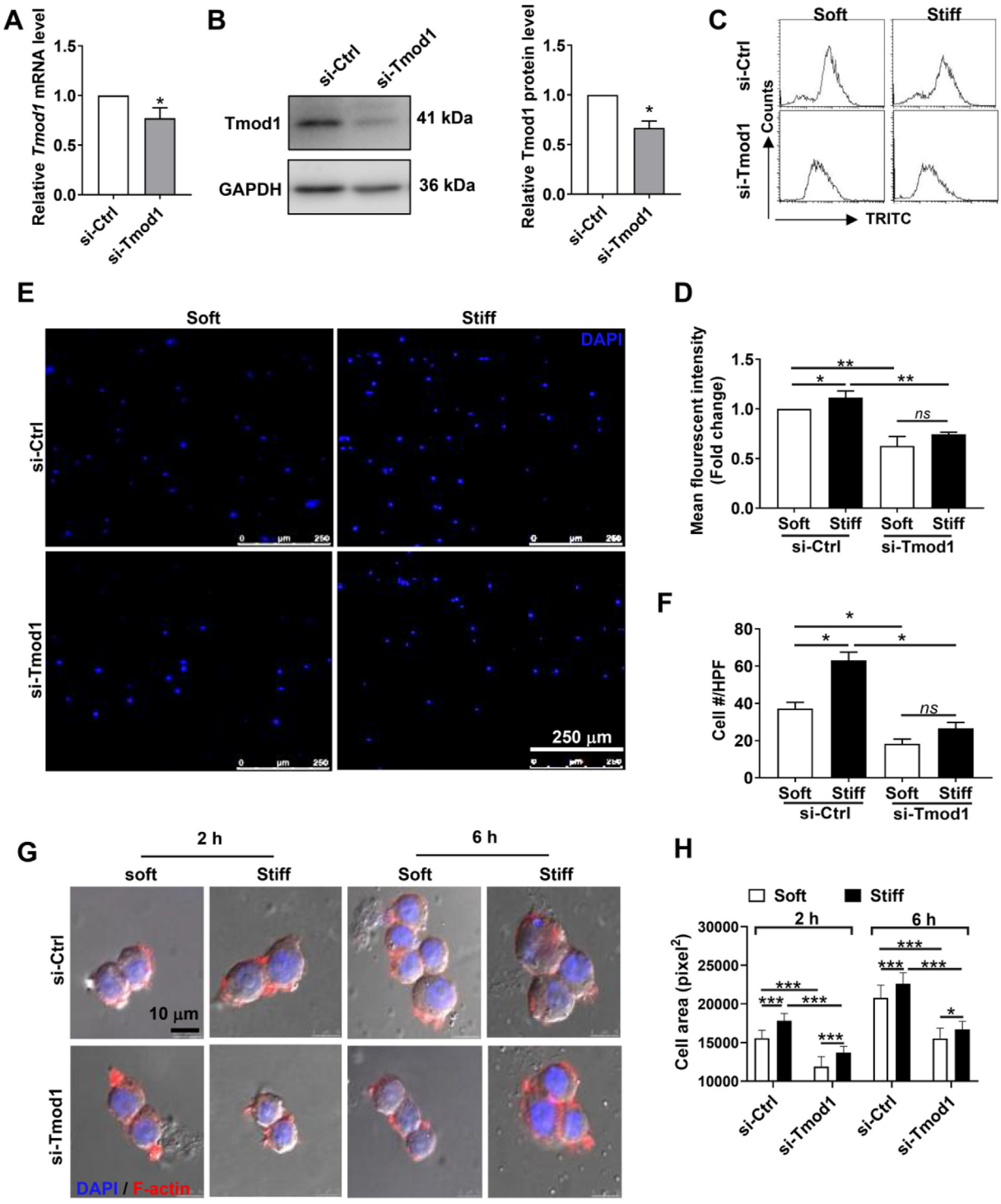

Fig. 3. Deficiency of Tmod1 in macrophages eliminates the changes in actin polymerization, cell adhesion and spreading induced by stiff matrix. (A–B) The validation of Tmod1 expression in Raw264.7 cells transfected with siRNA targeting Tmod1 (si-Tmod1) and control siRNA (si-control) at mRNA **(A)** and protein **(B)** levels by quantitative RT-PCR and western blotting. The representative blots were shown in the left panel of **(B)** and the semi-quantification data was shown in the right panel of **(B)**. n = 3–4 biological replicates. **(C–D)** The flow cytometry analysis on actin polymerization in Raw264.7 cells transfected with si-control or si-Tmod1 and cultured on soft (2 kPa) and stiff (20 kPa) PA gels. The cells were stained with TRITC phalloidin. The representative flow cytometry plots were shown in **(C)** and the fold changes in mean fluorescence intensity were shown in **(D)**. n = 4 biological replicates. **(E–F)** The adhesion of Raw264.7 cells transfected with si-control or si-Tmod1 on soft and stiff PA gels. The adhered cells were stained with DAPI. The representative images were taken and shown in **(E)**. The cell numbers per high power field (HPF) were shown in **(F)**. n = 4 HPFs from 3 biological replicates. **(G–H)** The spreading of Raw264.7 cells transfected with si-control or si-Tmod1 on soft and stiff PA gels for 2 and 6 h. The cells were stained with TRITC phalloidin and pictures were taken on a differential interference contrast (DIC) microscope. The representative images were shown in **(G)**. The cell areas were measured with Image J software and shown in **(H)**. n = 16 cells from 3 biological replicates. Data in **(A)** and **(B)** were analyzed by Student's *t*-test. Data in **(D)**, **(F)**, and **(H)** were analyzed by two-way ANOVA test followed by the Tukey's multiple comparisons test. *: $P < 0.05$, **: $P < 0.01$, ***: $P < 0.001$, ns: no significance.

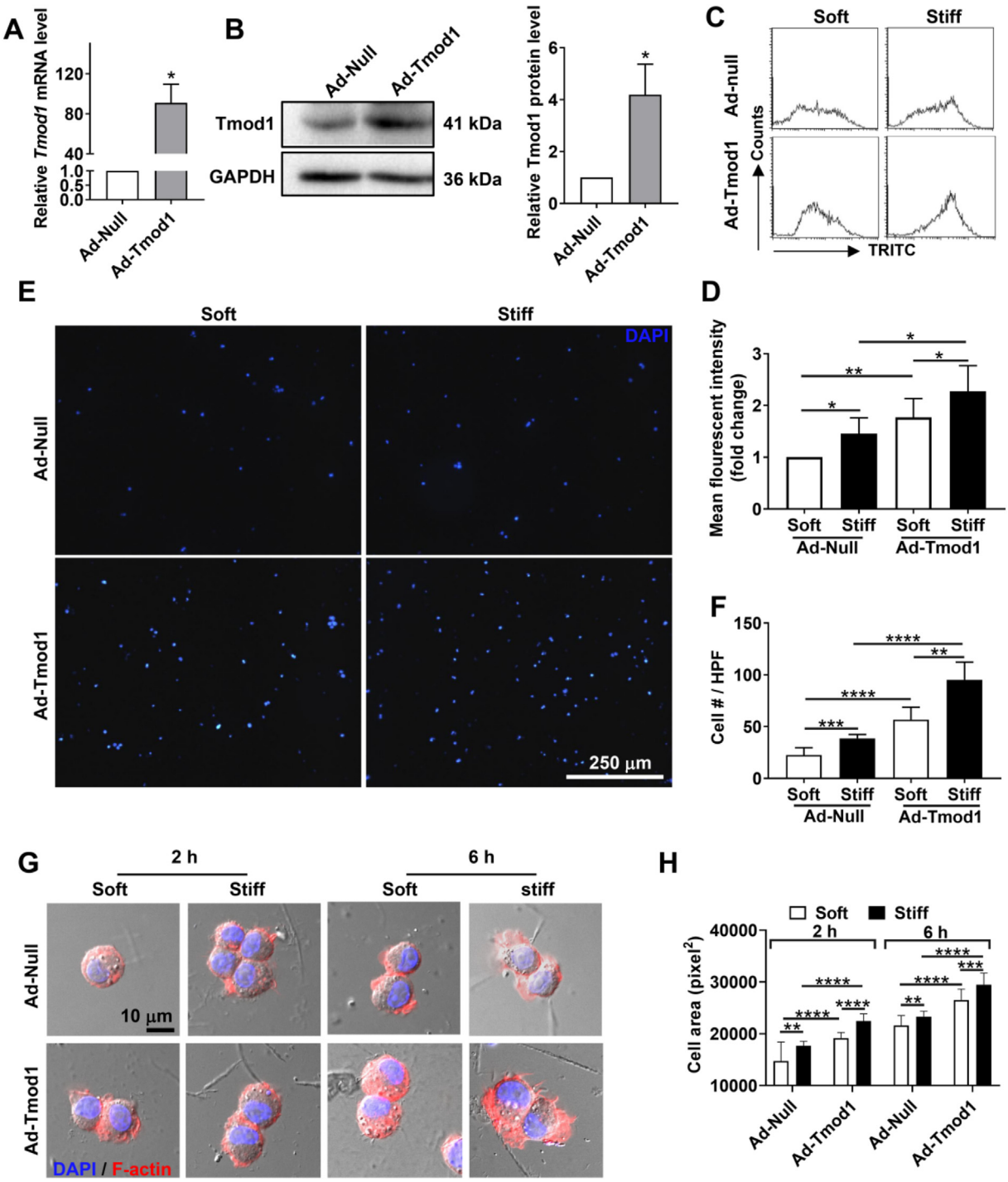

Fig. 4. Overexpression of Tmod1 in macrophages enhances actin polymerization, cell adhesion and spreading on stiff matrix. (A–B) The validation of Tmod1 expression in Raw264.7 cells infected with adenovirus expressing Tmod1 (Ad-Tmod1) and control adenovirus (Ad-null) at mRNA **(A)** and protein **(B)** levels by quantitative RT-PCR and western blotting. The representative blots were shown in the left panel of **(B)** and the semi-quantification data was shown in the right panel of **(B)**. n = 3 biological replicates. **(C–D)** The flow cytometry analysis on actin polymerization in Raw264.7 cells infected with Ad-null or Ad-Tmod1 and cultured on soft (2 kPa) and stiff (20 kPa) PA gels. The cells were stained with TRITC phalloidin. The representative flow cytometry plots were shown in **(C)** and the fold changes in mean fluorescence intensity were shown in **(D)**. n = 5 biological replicates. **(E–F)** The adhesion of Raw264.7 cells infected with Ad-null or Ad-Tmod1 on soft and stiff PA gels. The adhered cells were stained with DAPI. The representative images were taken and shown in **(E)**. The cell numbers per high power field (HPF) were shown in **(F)**. n = 5–9 HPFs from 3 biological replicates. **(G–H)** The spreading of Raw264.7 cells infected with Ad-null or Ad-Tmod1 on PA gels with 2 and 20 kPa stiffness for 2 and 6 h. The cells were stained with TRITC phalloidin and pictures were taken on a differential interference contrast (DIC) microscope. The representative images were shown in **(G)**. The cell areas were measured with Image J software and shown in **(H)**. n = 13–16 cells from 3 biological replicates. Data in **(A)** and **(B)** were analyzed by Student's *t*-test. Data in **(D)**, **(F)**, and **(H)** were analyzed by two-way ANOVA test followed by the Tukey's multiple comparisons test. *: $P < 0.05$, **: $P < 0.01$, ***: $P < 0.001$, ****: $P < 0.0001$, ns: no significance.

3.5. Tmod1 regulates the expression of vinculin and formation of focal adhesion in macrophages

We observed that Tmod1 participated in cell adhesion, spreading and podosome formation in macrophages cultured on stiff matrix. Focal adhesions mediate cell adhesion by connecting the cytoskeleton to the extracellular matrix and are essential for cell migration.[26,27] Therefore, we examined the effect of Tmod1 on a critical component in focal adhesion, vinculin, in macrophages. By western blotting, we found that stiff matrix could significantly upregulate the expression of vinculin compared to soft matrix (Fig. 5A). We overexpressed Tmod1 by transfecting Raw264.7 cells with Tmod1-DDK plasmid and prepared peritoneal macrophages from wild type and *TOT/Tmod1*$^{-/-}$ mice. Quantitative PCR and western blotting data showed that overexpression of Tmod1 caused the upregulation of vinculin in macrophages, while Tmod1 deficiency resulted in the downregulation of vinculin (Fig. 5B-D). The results suggest that both stiff matrix and Tmod1 could regulate the expression of vinculin, thus the formation of focal adhesion.

We then performed immunostaining to detect vinculin positive focal adhesion. We found that on stiff matrix, macrophages formed more focal adhesions, which was consistent with Western blot data. When Tmod1 was overexpressed, the numbers of vinculin positive focal adhesion increased in macrophages cultured on both soft and stiff matrix (Fig. 5E and F). Tmod1 overexpressing macrophages cultured on stiff matrix had the highest number of focal adhesions. When Tmod1 was deficient, the numbers of vinculin positive focal adhesion were significantly decreased in macrophages on both soft and stiff matrix, but there were still more focal adhesions formed on stiff matrix than on soft matrix (Fig. 5G and H). The data suggest that Tmod1 could regulate the expression of vinculin and participated in the formation of focal adhesion in macrophages induced by stiff matrix.

3.6. The deficiency of Tmod1 in macrophages retards the formation of atherosclerotic plaques in stiff blood vessels

Monocyte and macrophage infiltration is the key step in the development of atherosclerosis. Since Tmod1 appeared to play an important role in macrophage rigidity and migration on stiff matrix, we hypothesized that Tmod1 in macrophages would affect the atherosclerotic plaques in blood vessels with different stiffness. To test our hypothesis, we performed bone marrow transplantation and BAPN injection in *ApoE*$^{-/-}$ mice. We transplanted bone marrow cells from wild type or *TOT/Tmod1*$^{-/-}$ mice to lethally irradiated *ApoE*$^{-/-}$ mice. After bone marrow reconstitution, the mice were injected with BAPN (to lower the stiffness of blood vessels) or PBS for 8 weeks. The body weight was monitored every week and there were no significant difference among the groups (Fig. 6A). At the end of week 8, the mice were sacrificed and the size of atherosclerotic plaques in aortic root was analyzed. The data showed that in mice transplanted with wild type bone marrow cells, the size of plaques was much larger in PBS group (with higher stiffness) than in BAPN group (with lower stiffness) ($P = 0.1005$, Fig. 6B and C). In mice that were injected with BAPN, transplantation of wild type or Tmod1-deficient bone marrow cells resulted in comparable size of atherosclerotic plaques. But in mice that were injected with PBS, transplantation of Tmod1-deficent bone marrow cells led to significantly reduced plaque size as compared to transplantation of wild type bone marrow cells (Fig. 6B and C). To exclude the effect of lipids, we detected the levels of total cholesterol and triglyceride in the plasma of mice. The results showed that they were comparable in mice transplanted with bone marrow cells from wild type and *TOT/Tmod1*$^{-/-}$ mice (Fig. 6D and E). These results suggest that the deficiency of Tmod1 in macrophages retarded the formation of atherosclerotic plaques in stiff blood vessels.

4. Discussion

Arteries undergo stiffening with normal aging and the stiffening process is exaggerated by metabolic syndromes and diabetes.[28,29] The alteration in arterial stiffness is one of the earliest detectable manifestations of adverse vascular remodeling[11] and arterial stiffness is a cholesterol-independent risk factor for a first cardiovascular event.[30] The development of atherosclerosis results in the increased stiffness in arteries.[13] Therefore, arterial stiffening is not only a cause but also a consequence of cardiovascular disease. Monocyte/macrophage infiltration into the vascular wall is the key step in atherosclerosis. The circulating monocytes adhere to endothelial cells and begin the process of macrophage differentiation and transmigrate into the subendothelial spaces. The subendothelial macrophages develop into foam cells that populate lesions. Thus, the mechanical behaviors of monocytes and macrophages would be influenced by the arterial stiffness at both early and later stages of atherosclerosis.

In the present study, we investigated macrophage rigidity and migration ability on PA gels with 2 kPa and 20 kPa stiffness, which correspond to the stiffness of healthy and diseased blood vessels. We found that compared to soft matrix (2 kPa), stiff matrix (20 kPa) caused the increase in macrophage rigidity and promoted macrophage migration (Fig. 1). Consistently, transcriptional analysis showed that the genes related to positive regulation of cell migration were upregulated on stiff substrate. Researchers studied monocyte/macrophage migration on 2D surface or 3D matrix with various stiffness.[16–18,31,32] Sridharan et al. found that stiff PA gels (323 kPa) primed THP-1 derived macrophages towards a pro-inflammatory phenotype with lower migration ability, while soft (11 kPa) and medium (88 kPa) stiffness gels primed cells towards an anti-inflammatory phenotype with higher migration ability.[17] With bone marrow-derived macrophages (BMDMs), Chen et al. found that low substrate stiffness (2.55 kPa) promoted BMDMs to shift to classically activated macrophages (M1), while middle (34.88 kPa) stiffness promoted BMDMs to shift to alternatively activated macrophages (M2).[31] It was shown that M1 macrophages had significantly impaired migration velocity compared to M2 macrophages.[17] These published works and our data suggest that there might be a “biphasic” change in macrophage migration depending on the matrix stiffness, i.e., the migration ability of macrophages is low on substrate with ~2 kPa stiffness, becomes high on substrate with ~11–88 kPa stiffness, but decreases again on substrate with over 300 kPa stiffness. This could well explain the distinct behaviors of macrophages seen in different scenes, such as vascular stiffening, atherosclerosis, tissue repair, biomaterial implantation, and osteogenesis.

Macrophages could adopt two migration modes like tumor cells: one is Rho-A kinase (ROCK)-dependent, podosome-independent amoeboid migration mode; the other one is a ROCK-independent, podosome-dependent mesenchymal migration mode.[17,33,34] Based on our observation, macrophages cultured on stiff matrix (20 kPa) tended to spread larger and have more podosomes and vinculin positive focal adhesions (Figs. 4 and 5). Considering the higher migration ability in macrophages cultured on stiff matrix, we think the cells most likely adopted a mesenchymal migration mode.

Actin polymerization is a major determinant for macrophage rigidity and migration. As an actin capping protein, Tmod1 plays an important role in actin polymerization. We found that Tmod1 was upregulated by stiff matrix and participated in actin polymerization, cell adhesion, cell spreading of macrophages induced by stiff matrix. The knockdown of Tmod1 in macrophages eliminated the difference in actin polymerization and cell adhesion between soft and stiff matrix (Fig. 3). This indicates that Tmod1 should be essential in determining the macrophage rigidity and be important in macrophage migration on stiff matrix. The role of Tmod1 in macrophages was well demonstrated in our animal study (Fig. 6). In *ApoE*$^{-/-}$ mice with softened vessels by BAPN, there was no difference in the sizes of atherosclerotic plaques no matter whether Tmod1 was absent or not in macrophages. But in *ApoE*$^{-/-}$ mice with stiff vessels, the knockout of Tmod1 in macrophages greatly reduced sizes of atherosclerotic plaques, suggesting less macrophage infiltration occurred when Tmod1 was absent.

In cardiomyocytes, researchers found that overexpression of Tmod1 caused the phosphorylation and redistribution of paxillin,[22] suggesting that Tmod1 is involved in the assembly of focal adhesion. Consistently,

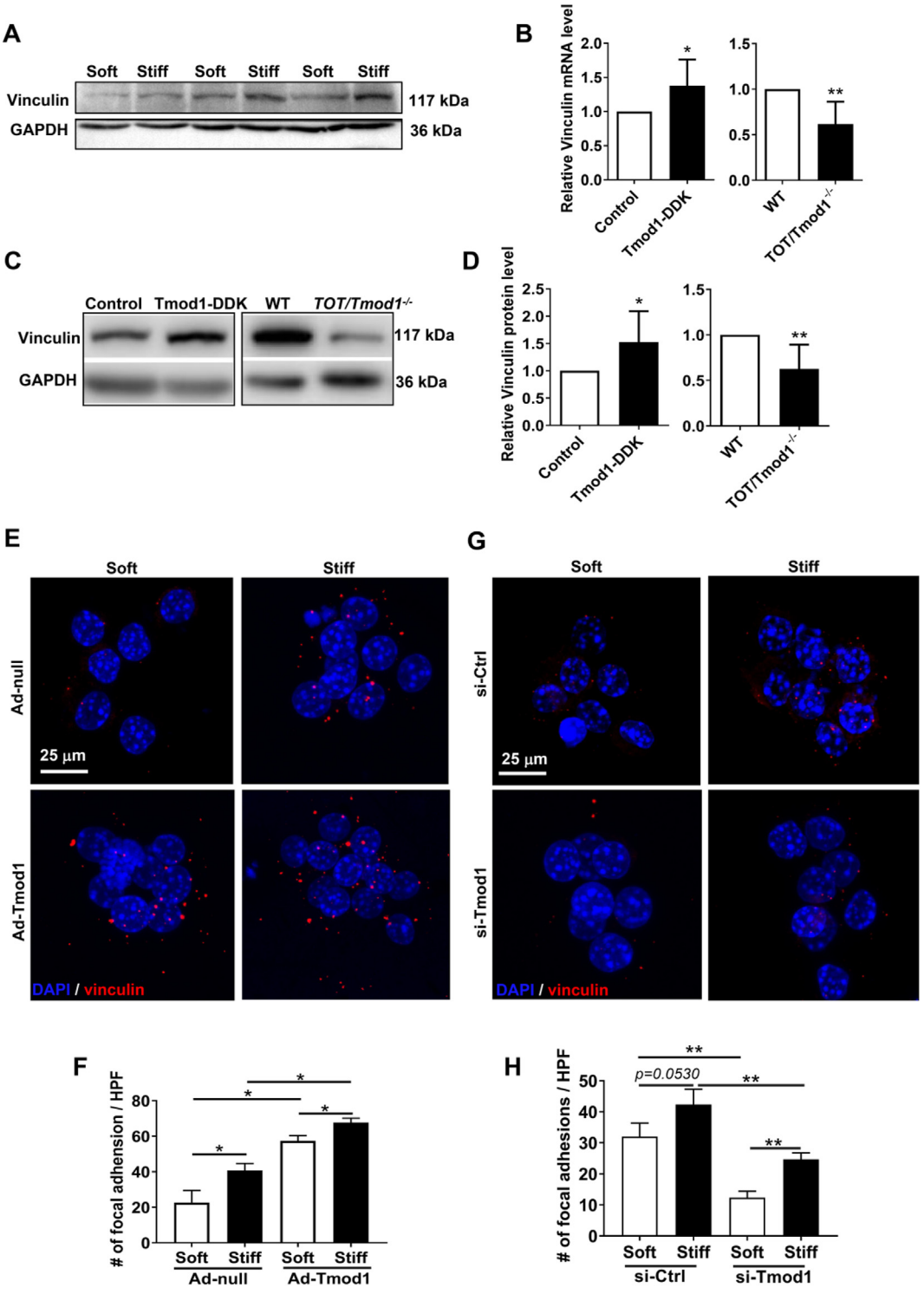

Fig. 5. Tmod1 regulates the expression of vinculin and formation of focal adhesion in macrophages. (A) The detection of vinculin expression by western blotting in Raw264.7 cells cultured on soft (2 kPa) and stiff (20 kPa) PA gels. The blots with 3 biological replicates were shown. **(B–D)** The mRNA **(B)** and protein **(C–D)** levels of vinculin in Raw264.7 cells transfected with Tmod1-DDK plasmid and peritoneal macrophages isolated from wild type (WT) or *TOT/Tmod1*$^{-/-}$ mice. The representative blots were shown in **(C)** and the semi-quantification data was shown in **(D)**. n = 6–9 biological replicates. **(E–F)** The immunostaining of vinculin in Raw264.7 cells infected with Ad-null or Ad-Tmod1 and cultured on soft and stiff PA gels. The nuclei were counterstained with DAPI. The representative images were shown in **(E)**. The numbers of vinculin positive focal adhesions per high power field (HPF) were counted and presented in **(F)**. n = 3 HPFs from 3 biological replicates. **(G–H)** The immunostaining of vinculin in Raw264.7 cells transfected with si-control or si-Tmod1 and cultured on soft and stiff PA gels. The nuclei were counterstained with DAPI. The representative images were shown in **(G)**. The numbers of vinculin positive focal adhesions per high power field (HPF) were counted and presented in **(H)**. n = 3 HPFs from 3 biological replicates. Data in **(B)** and **(D)** were analyzed by Student's *t*-test. Data in **(F)** and **(H)** were analyzed by two-way ANOVA test followed by the Tukey's multiple comparisons test. *: $P < 0.05$, **: $P < 0.01$.

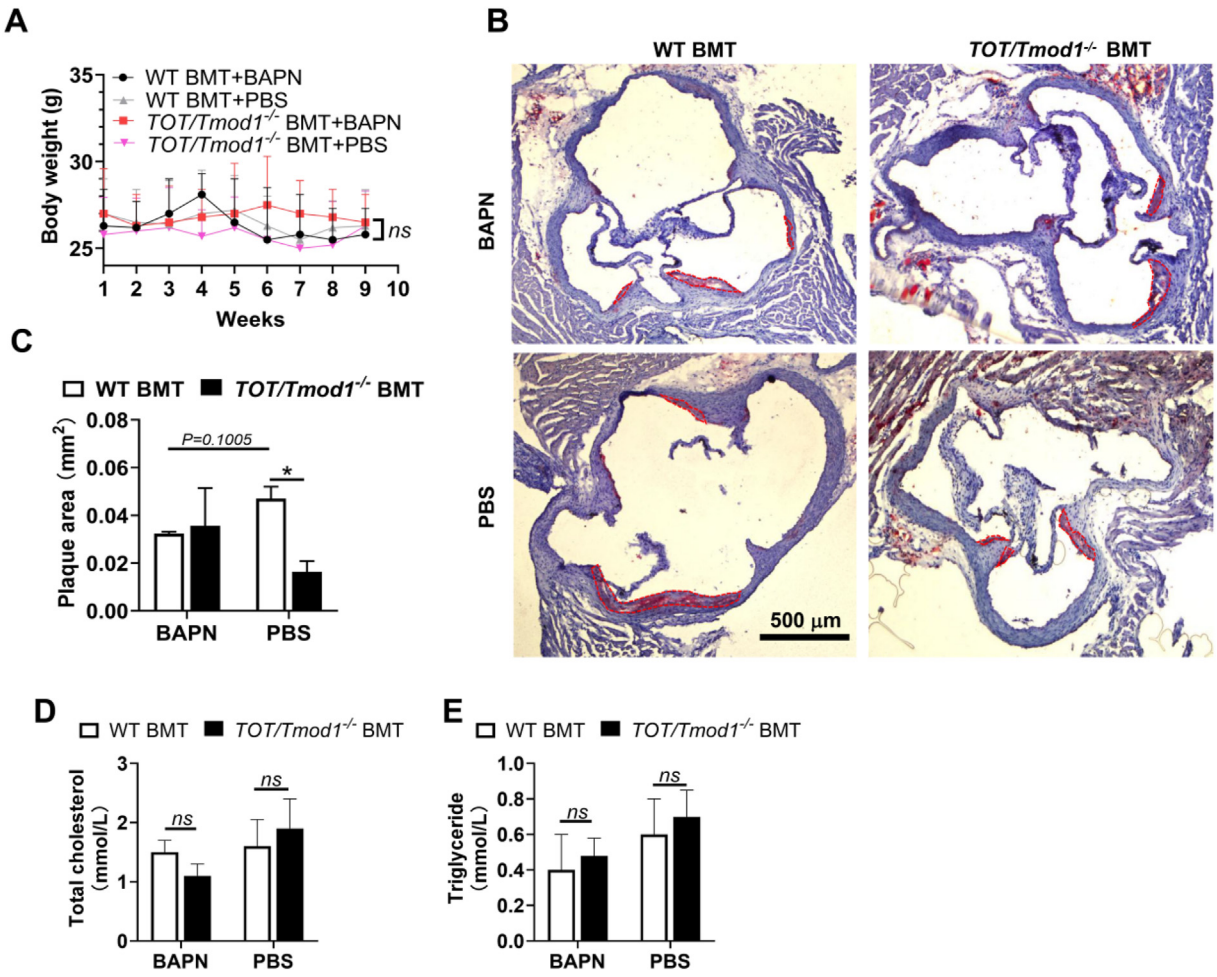

Fig. 6. The deficiency of Tmod1 in macrophages retards the formation of atherosclerotic plaques in stiff blood vessels. (A) The body weights of *ApoE*$^{-/-}$ mice that were transplanted with bone marrow cells from wild type (WT) or *TOT/Tmod1*$^{-/-}$ mice and then treated with PBS or lysyl oxidase inhibitor BAPN for 8 weeks. **(B)** The images of oil red O staining of aortic roots from *ApoE*$^{-/-}$ mice with bone-marrow transplantation and PBS or BAPN treatment. The sections were counterstained with hematoxylin. The atherosclerotic plaques were highlighted with red dotted lines. **(C)** The plaque areas were manually measured by Image J software. n = 3–5 mice. **(D–E)** The levels of total cholesterol **(D)** and triglyceride **(E)** in mice with bone-marrow transplantation and PBS or BAPN treatment. Data was analyzed by two-way ANOVA test followed by the Tukey's multiple comparisons test. *: $P < 0.05$, ns: no significance.

we found that Tmod1 also participated the formation of focal adhesion in macrophages when cultured on stiff matrix. It was also noticed that when we manipulated Tmod1 expression in macrophages, the expression of vinculin changed accordingly. Higher Tmod1 level corresponded to higher vinculin expression (Fig. 5). In our preliminary data, we also found that Tmod1 also seemed to regulate the expression of integrin β1 (data not shown). Importantly, vinculin expression was upregulated by stiff matrix, suggesting that it was mechanosensitive. It was shown that macrophage mechanosensing is mediated by cytoskeletal remodeling and cytoskeletal dynamics could integrate biochemical signaling and ultimately regulate chromatin accessibility to control the mechanosensitive gene expression program.[32] Therefore, it is reasonable to infer that Tmod1 may regulate the mechanosensing of macrophage and gene expression program by changing cytoskeletal dynamics.

There is evidence that Piezo-type mechanosensitive ion channel component 1 (Piezo1) and transient receptor potential cation channel, subfamily V, member 4 (TRPV4) are involved in sensing substrate stiffness on 2D surfaces.[35,36] The positive feedback exists between actin polymerization and Piezo1-mediated calcium influx in macrophages, which regulates the activation and mechanosensing of stiffness in macrophages.[35] Our recent work showed that Tmod1 could affect the calcium influx in macrophages upon lipopolysaccharide (LPS) treatment.[37] It would be interesting to study whether there is any crosstalk between Tmod1 and Piezo1 in regulating macrophage migration on stiff matrix.

In vascular smooth muscle cells (VSMCs), researchers found that the effects of matrix stiffness on VSMCs greatly depended on the biochemical properties of the matrix and there was a "stiffness-by-ligand" effect.[12] However, evidence showed that macrophages were capable of responding to substrate stiffness irrespective of the matrix proteins being presented to them.[17] In addition to the matrix proteins, other biochemical cues exist in the microenvironment that macrophages are in. In atherosclerotic lesions, modified low density lipoproteins (LDL), such as oxidized LDLs (oxLDL), are accumulated. It has been shown that oxLDL inhibits the migration of macrophages via CD36-mediated signaling pathways.[38] Therefore, there may exist a crosstalk between the physical cues (e.g., matrix stiffness) and biochemical cues (e.g., oxLDL). These factors may synergistically regulate macrophage behavior in diseased blood vessels and need to be studied further.

In conclusion, we demonstrated that matrix stiffness in diseased blood vessels increased macrophage rigidity and promoted macrophage migration and the cytoskeletal protein Tmod1 was a key regulator in these processes. Our work will help us to understand the biomechanical mechanisms for the development of atherosclerosis and provide new angles in prevention and treatment of atherosclerotic cardiovascular diseases.

CRediT authorship contribution statement

Yajun Meng: Writing – original draft, Validation, Methodology, Investigation, Formal analysis, Data curation. **Amannisa Tuersuntuoheti:** Methodology, Investigation, Data curation. **Siyu Jiang:** Investigation, Formal analysis, Data curation. **Jiayi Xie:** Software, Methodology, Investigation. **Zejun Yue:** Validation, Software, Methodology, Investigation. **Dingwen Xu:** Validation, Software, Methodology. **Xueyu Geng:** Software, Methodology, Investigation, Formal analysis. **Xiang Lian:** Validation, Software, Methodology. **Lide Xie:** Supervision, Project administration. **Lanping Amy Sung:** Supervision, Project administration, Conceptualization. **Xifu Wang:** Supervision, Project administration, Funding acquisition, Conceptualization. **Jing Zhou:** Visualization, Supervision, Project administration, Conceptualization. **Weijuan Yao:** Writing – review & editing, Writing – original draft, Visualization, Validation, Supervision, Software, Project administration, Funding acquisition, Formal analysis, Data curation, Conceptualization.

Ethical approval

All the animal experiments for the study were performed following standards according to the protocol approved by the Animal Care Committee of Peaking University Health Science Center (No. HL2021172).

Declaration of competing interest

The authors declare that there are no competing financial interests in relation to this work.

Acknowledgements

This work was supported by National Natural Science Foundation of China (Nos. 31570938, 32171143, and 31771280 to W.Y.) and Natural Science Foundation of Beijing (No. 7232042 to X.W.).

References

1. Yang X, Li J, Hu D, et al. Predicting the 10-year risks of atherosclerotic cardiovascular disease in Chinese population. *Circulation*. 2016;134(19):1430–1440. https://doi.org/10.1161/circulationaha.116.022367.
2. Cheng TO. Cardiovascular health, risks and diseases in contemporary China. *Int J Cardiol*. 2012;154(2):233–242. https://doi.org/10.1016/j.ijcard.2011.12.023.
3. Lechner K, von Schacky C, McKenzie AL, et al. Lifestyle factors and high-risk atherosclerosis: pathways and mechanisms beyond traditional risk factors. *European Journal of Preventive Cardiology*. 2019;27(4):394–406. https://doi.org/10.1177/2047487319869400.
4. Silverstein RL, Febbraio M. CD36 and atherosclerosis. *Curr Opin Lipidol*. 2000;11(5):483–491. https://doi.org/10.1097/00041433-200010000-00006.
5. Curtiss LK. Reversing atherosclerosis? *N Engl J Med*. 2009;360(11):1144–1146. https://doi.org/10.1056/NEJMcibr0810383.
6. Trogan E, Feig JE, Dogan S, et al. Gene expression changes in foam cells and the role of chemokine receptor CCR7 during atherosclerosis regression in ApoE-deficient mice. *Proc Natl Acad Sci USA*. 2006;103(10):3781–3786. https://doi.org/10.1073/pnas.0511043103.
7. Mierke CT. The fundamental role of mechanical properties in the progression of cancer disease and inflammation. *Rep Prog Phys*. 2014;77(7). https://doi.org/10.1088/0034-4885/77/7/076602.
8. Zeng W, Shi Y, Deng X. Viscoelastic properties of phagocytes in arteriosclerotic origin. *Appl Mech Mater*. 2014;540:321–325.
9. Kothapalli D, Liu S-L, Bae Yong H, et al. Cardiovascular protection by ApoE and ApoE-HDL linked to suppression of ECM gene expression and arterial stiffening. *Cell Rep*. 2012;2(5):1259–1271. https://doi.org/10.1016/j.celrep.2012.09.018.
10. Ballotta V, Driessen-Mol A, Bouten CVC, Baaijens FPT. Strain-dependent modulation of macrophage polarization within scaffolds. *Biomaterials*. 2014;35(18):4919–4928. https://doi.org/10.1016/j.biomaterials.2014.03.002.
11. Barallobre-Barreiro J, Loeys B, Mayr M, Rienks M, Verstraeten A, Kovacic JC. Extracellular matrix in vascular disease, Part 2/4. *J Am Coll Cardiol*. 2020;75(17):2189–2203. https://doi.org/10.1016/j.jacc.2020.03.018.
12. Sazonova OV, Isenberg BC, Herrmann J, et al. Extracellular matrix presentation modulates vascular smooth muscle cell mechanotransduction. *Matrix Biol*. 2015;41:36–43. https://doi.org/10.1016/j.matbio.2014.11.001.
13. Xie S-A, Zhang T, Wang J, et al. Matrix stiffness determines the phenotype of vascular smooth muscle cell in vitro and in vivo: role of DNA methyltransferase 1. *Biomaterials*. 2018;155:203–216. https://doi.org/10.1016/j.biomaterials.2017.11.033.
14. Jensen LF, Bentzon JF, Albarrán-Juárez J. The phenotypic responses of vascular smooth muscle cells exposed to mechanical cues. *Cells*. 2021;10(9). https://doi.org/10.3390/cells10092209.
15. Féréol S, Fodil R, Labat B, et al. Sensitivity of alveolar macrophages to substrate mechanical and adhesive properties. *Cell Motil Cytoskelet*. 2006;63(6):321–340. https://doi.org/10.1002/cm.20130.
16. Patel NR, Bole M, Chen C, et al. Cell elasticity determines macrophage function. *PLoS ONE*. 2012;7(9). https://doi.org/10.1371/journal.pone.0041024.
17. Sridharan R, Cavanagh B, Cameron AR, Kelly DJ, O'Brien FJ. Material stiffness influences the polarization state, function and migration mode of macrophages. *Acta Biomater*. 2019;89:47–59. https://doi.org/10.1016/j.actbio.2019.02.048.
18. Adebowale K, Ha B, Saraswathibhatla A, et al. Monocytes use protrusive forces to generate migration paths in viscoelastic collagen-based extracellular matrices. *bioRxiv Prepr*. 2023. https://doi.org/10.1101/2023.06.09.544394, 2023.06.09.544394.
19. Sung LA, Lin JJC. Erythrocyte tropomodulin binds to the N-terminus of hTM 5, a tropomyosin isoform encoded by the γ-tropomyosin gene. *Biochem Biophys Res Commun*. 1994;201(2):627–634. https://doi.org/10.1006/bbrc.1994.1747.
20. Chu X, Chen J, Reedy MC, Vera C, Sung KLP, Sung LA. E-Tmod capping of actin filaments at the slow-growing end is required to establish mouse embryonic circulation. *Am J Physiol Heart Circ Physiol*. 2003;284(5):H1827–H1838. https://doi.org/10.1152/ajpheart.00947.2002.
21. Green T, Vera C, Sussman MA, Martone M, Sung LA. Mechanobiology of erythrocytes from adult mice homozygous for a targeted disruption of the E-Tmod gene at exon 1. *Cell Mol Bioeng*. 2011;4:637–647.
22. Melendez J, Welch S, Schaefer E, et al. Activation of pyk2/related focal adhesion tyrosine kinase and focal adhesion kinase in cardiac remodeling. *J Biol Chem*. 2002;277(47):45203–45210. https://doi.org/10.1074/jbc.M204886200.
23. Tse JR, Engler AJ. Preparation of hydrogel substrates with tunable mechanical properties. *Curr Protoc Cell Biol*. 2010;47(1). https://doi.org/10.1002/0471143030.cb1016s47.
24. Schindelin J, Arganda-Carreras I, Frise E, et al. Fiji: an open-source platform for biological-image analysis. *Nat Methods*. 2012;9(7):676–682. https://doi.org/10.1038/nmeth.2019.
25. Rezvani-Sharif A, Tafazzoli-Shadpour M, Avolio A. Progressive changes of elastic moduli of arterial wall and atherosclerotic plaque components during plaque development in human coronary arteries. *Med Biol Eng Comput*. 2018;57(3):731–740. https://doi.org/10.1007/s11517-018-1910-4.
26. Legerstee K, Houtsmuller A. A layered view on focal adhesions. *Biology*. 2021;10(11). https://doi.org/10.3390/biology10111189.
27. Yamaguchi N, Knaut H. Focal adhesion-mediated cell anchoring and migration: from in vitro to in vivo. *Development*. 2022;149(10). https://doi.org/10.1242/dev.200647.
28. Lakatta EG. Central arterial aging and the epidemic of systolic hypertension and atherosclerosis. *Journal of the American Society of Hypertension*. 2007;1(5):302–340. https://doi.org/10.1016/j.jash.2007.05.001.
29. Stehouwer CDA, Henry RMA, Ferreira I. Arterial stiffness in diabetes and the metabolic syndrome: a pathway to cardiovascular disease. *Diabetologia*. 2008;51(4):527–539. https://doi.org/10.1007/s00125-007-0918-3.
30. Mitchell GF, Hwang S-J, Vasan RS, et al. Arterial stiffness and cardiovascular events. *Circulation*. 2010;121(4):505–511. https://doi.org/10.1161/circulationaha.109.886655.
31. Chen M, Zhang Y, Zhou P, et al. Substrate stiffness modulates bone marrow-derived macrophage polarization through NF-κB signaling pathway. *Bioact Mater*. 2020;5(4):880–890. https://doi.org/10.1016/j.bioactmat.2020.05.004.
32. Meizlish ML, Kimura Y, Pope SD, et al. Mechanosensing regulates tissue repair program in macrophages. *Sci Adv*. 2024;10(11). https://doi.org/10.1126/sciadv.adk6906.
33. Friedl P, Wolf K. Tumour-cell invasion and migration: diversity and escape mechanisms. *Nat Rev Cancer*. 2003;3(5):362–374. https://doi.org/10.1038/nrc1075.
34. Van Goethem E, Poincloux R, Gauffre F, Maridonneau-Parini I, Le Cabec V. Matrix architecture dictates three-dimensional migration modes of human macrophages: differential involvement of proteases and podosome-like structures. *J Immunol*. 2010;184(2):1049–1061. https://doi.org/10.4049/jimmunol.0902223.
35. Atcha H, Jairaman A, Holt JR, et al. Mechanically activated ion channel Piezo1 modulates macrophage polarization and stiffness sensing. *Nat Commun*. 2021;12(1). https://doi.org/10.1038/s41467-021-23482-5.
36. Scheraga RG, Abraham S, Niese KA, et al. TRPV4 mechanosensitive ion channel regulates lipopolysaccharide-stimulated macrophage phagocytosis. *J Immunol*. 2016;196(1):428–436. https://doi.org/10.4049/jimmunol.1501688.
37. Geng X, Xia X, Liang Z, et al. Tropomodulin1 exacerbates inflammatory response in macrophages by negatively regulating LPS-induced TLR4 endocytosis. *Cell Mol Life Sci*. 2024;81(1). https://doi.org/10.1007/s00018-024-05424-8.
38. Park YM, Febbraio M, Silverstein RL. CD36 modulates migration of mouse and human macrophages in response to oxidized LDL and may contribute to macrophage trapping in the arterial intima. *J Clin Investig*. 2008. https://doi.org/10.1172/jci35535.